Origin of polar nanoregions in relaxor ferroelectrics: Nonlinearity, discrete breather formation, and charge transfer

J. Macutkevic,[1] J. Banys,[1] A. Bussmann-Holder,[2] and A. R. Bishop[3]
[1]*Faculty of Physics, Vilnius University, Sauletekio 9, LT-10222 Vilnius, Lithuania*
[2]*Max Planck Institute for Solid State Research, Heisenbergstrasse 1, D-70569 Stuttgart, Germany*
[3]*Los Alamos National Laboratory, Theoretical Division, Los Alamos, New Mexico 87545, USA*
(Received 28 January 2011; revised manuscript received 18 March 2011; published 16 May 2011; publisher error corrected 2 June 2011)

A central issue in the physics of relaxor ferroelectrics is the origin of the formation of polar nanoregions below some characteristic temperature scale. While it is often attributed to chemical disorder, random bond–random field appearance, or local symmetry lowering, it is shown here that the huge intrinsic nonlinearity of ferroelectrics gives rise to spatially limited excitations of discrete breather (DB) type, which interact strongly and self-consistently with the remaining lattice. This scenario corresponds to a two-component approach to relaxor physics with distinctive signatures in the dielectric spectra and strong charge-transfer effects. The theoretical results are compared to broadband dielectric spectroscopy on 0.2PSN-0.4PMN-0.4PZN ceramics, which provides clear evidence for the two-component scenario and the emergence of DB-like dynamics with decreasing temperature.

DOI: 10.1103/PhysRevB.83.184301 PACS number(s): 77.22.−d, 63.20.−e, 78.30.−j

I. INTRODUCTION

Relaxor ferroelectricity is almost exclusively observed in systems with chemical disorder. While this feature poses challenges on the precise characterization of the samples, disorder can be tuned, and thereby, the physical properties can also be varied and enlarge considerably the application range. Typically, ABO_3-type ferroelectrics exhibit relaxor properties when the A or B sites are substituted by a proper cation. This observation was early claimed to be the origin of the observed diffuse phase transitions since chemical disorder might give rise to *local* phase transitions that do not mirror the bulk properties.[1] Later, it was suggested that polar nanoregions (PNR) form in relaxors, which stem from fluctuating dipole moments.[2–4] Direct experimental evidence for these PNR's is still missing; however, a variety of indirect observations support the PNR scenario.[5] These include particularly infrared and broadband spectroscopy,[6–8] enhanced diffuse inelastic scattering, inelastic and pulsed inelastic neutron scattering,[9–12] Raman spectroscopy,[13] x-ray scattering,[14] and NMR measurements.[15] All experiments demonstrate that at least two components coexist in relaxors that are characterized by different time and length scales. While formerly it was speculated that relaxor and displacive ferroelectric behavior originates from different physics, it has been shown that a crossover between both dynamics takes place upon properly doping a displacive system to a relaxor and vice versa.[16–20]

Theoretically, no clear consensus has been achieved. It is, however, agreed that the PNR's have a lower symmetry than the matrix in which they are embedded.[21] As such, an analogy between relaxors and dipolar glasses[22] has been proposed, leading to the random field Ising model[23] and the spherical random bond–random field model.[24] While this approach is rather phenomenological, extensions have been proposed to include pairwise interactions between neighboring doped ions in a random field.[25–27]

The coexistence of local and average structures constituting the relaxor lattice leads to an apparent breakdown of the translational invariance and requires new techniques beyond conventional theories based on plane-wave states.

II. BACKGROUND

Ferroelectrics, independent of their structure and composition, are known to be dominated by strong anharmonicity and nonlinearity, which gives rise to double-well potentials or potentials of even more complicated form. While frequently the resulting dynamical behavior is treated in a quasiharmonic approximation, namely, plane-wave states, it has been shown that intrinsic localized modes (ILM) and discrete breathers (DB)[20,28–30] are characteristic excitations of such systems realized in various physical situations. The problem of DB and ILM formation lies in the fact that their stability is only guaranteed as long as their energy is confined to a regime in the optic acoustic mode gap. However, when such a situation is realized, these nonlinear objects extract spectral weight from the normal lattice modes and appear as Einstein oscillators in a confined momentum space region that defines their length scales.

Within the polarizability model,[31–33] DB's have been observed that either split off from the optic mode spectrum or emerge from the acoustic modes.[20,28–30] In both cases they substantially modify the dynamical behavior of the matrix, lead to anomalies in the acoustic modes, and particularly influence the lattice dynamics temperature dependence.

As detailed in previous work, the nonlinear objects are not in isolation but interact through a superposition with the lattice plane-wave states.[20,28–30] This interaction enables charge transfer between the host matrix and the DB's, which shifts oscillator strength from the lattice to the DB. The situation is comparable to polaron formation since the DB moves with a considerable amount of charge through the lattice.

III. MODEL APPROACH

The nonlinear potential that is used here differs from conventional ones through the use of the polarizability coordinate $w = v - u$, where v is the shell displacement and u is that of the shell surrounding core: $V(w) = g_2 w^2 + g_4 w^4$, with $g_2 < 0$, $g_4 > 0$. Effectively, w represents a local dipole

moment.[34,35] DB solutions are only obtained as long as the spatial extent exceeds several lattice constants n_c from the DB center at site n. We identify here the DB extent with the size of the PNR's. A consequence of the finite spatial spread of the DB is that the nonlinear potential becomes site dependent since the nonlinearity varies as $\tilde{g}_4^{(n)} = g_4/[2(n-n_c)^2]$. At the DB center the dipole moment is large for large n_c and reduced for small n_c. Upon approaching the border n_c of the PNR's, the local dipole is reduced to zero at $n = n_c$. This means that, within the spatial extent of the PNR's, not a single dipole moment is present but, rather, a spread of varying dipole moments that fluctuate and lead to an ill-defined structure within the PNR's, making the lowest symmetry the most likely one. Upon superposing matrix and DB displacements, a coupling between both is provided from which the lattice is stabilized, and the DB mode frequency adopts a temperature dependence. The coupled frequencies have to be derived self-consistently for each temperature T, which is complicated because the DB frequency is calculated from a third-order equation in the dipole moment that has to be iterated to convergence. In addition, the lattice mode follows a self-consistent loop where the DB dipoles enter. Note that the DB frequency depends not only on the magnitude of the dipole moment and the lattice mode frequency but also on the spatial extent of the DB through its dependence on n_c.

The complex dielectric function $\tilde{\varepsilon}(\omega)$ of the coupled system is calculated within standard theory:

$$\tilde{\varepsilon}(\omega) = \varepsilon_\infty + \sum_i S_i R_i(q,\omega_i), \tag{1}$$

where ω_i $(i = 1, 2)$ refer to the momentum q dependent optic lattice mode and the DB mode frequencies and $R_i(q,\omega)$ is the response function for the corresponding mode. In anharmonic crystals this is expressed as

$$R_i(q,\omega) = \left[\omega_i^2(q) - \omega^2 + 2\omega_i(q)\sum_i(q,\omega)\right]^{-1}, \tag{2}$$

with $\sum_i(q,\omega)$ being the self-energy. In the above case this energy relates directly to the integrated dipole moment, which is proportional to the self-consistently derived thermal average $\langle w^2\rangle_T = \sum_{q,i}\hbar w^2(q,i)/[m\omega_i(q)]\coth\frac{\hbar\omega_i(q)}{2kT}$. Since the DB mode frequency is dispersionless, the response function is calculated in the limit $q \to 0$. The calculated imaginary part of the dielectric permittivity is shown for small DB spatial extents and various temperatures in Fig. 1.

While at high temperatures the dielectric response is almost completely dominated by the lattice mode pseudoharmonic frequency, with decreasing temperature an additional peak develops on the low-frequency side that gains intensity at the expense of the lattice mode. Together with the intensity redistribution, an anomalous broadening of the lattice response sets in, whereas the DB mode sharpens. The appearance of the DB in the low-frequency regime suggests a strong DB acoustic mode coupling leading to enormous anomalies in the elastic constants, as observed experimentally.[36–42] Upon increasing the DB spatial extent, all the above-described features become much more pronounced (Fig. 2), and the DB mode dynamics slow down substantially. This has the consequence that the larger the PNR's are, the more they approach an almost-static

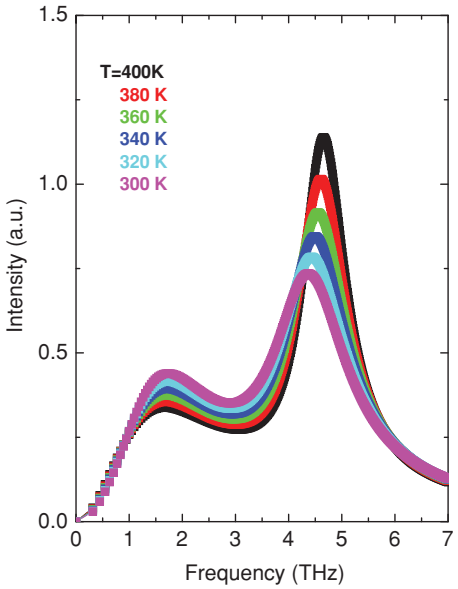

FIG. 1. (Color online) Temperature and frequency dependence of the breather mode response for fixed breather size. The choice of the size corresponds to the dilute doping limit.

limit where two time and length scales appear. Also, a much stronger piezoelectric coupling is present in the latter case, which could be the source of the enhanced piezoresponse reported for relaxor ferroelectrics.[5,43]

Since the DB stabilizes the lattice mode frequency, a soft mode-induced transition is suppressed, but only a minor (although still feasible) temperature dependence of the lattice mode remains [Fig. 3(a)], which is independent of the DB extent. Opposite to this finding, the DB mode frequency depends strongly on the DB spatial extent. As expected, it

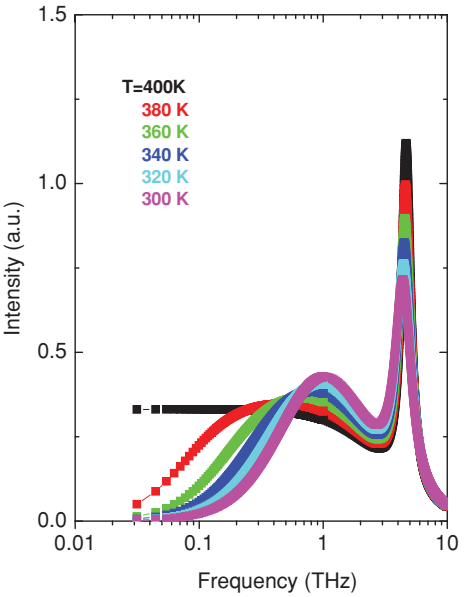

FIG. 2. (Color online) Temperature and frequency dependence of the breather mode response for fixed breather size. The choice of the size corresponds to the dense doping limit.

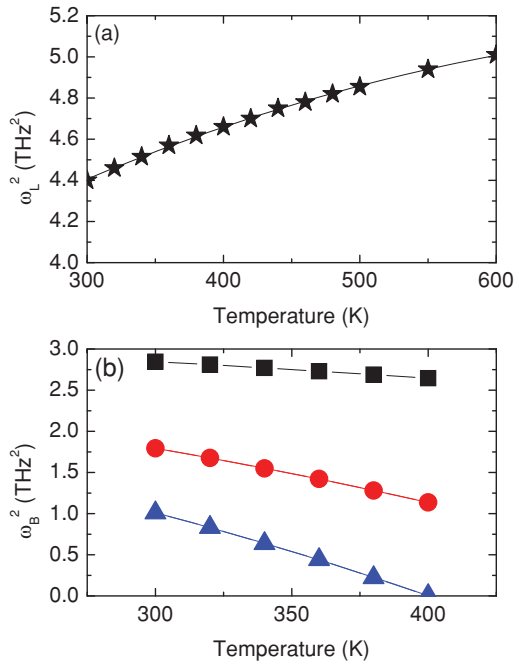

FIG. 3. (Color online) (a) Temperature dependence of the squared lattice mode frequency ω_L^2. (b) Temperature dependence of the squared breather mode frequency for the case of dilute doping (squares), intermediately dense doping (circles), and dense doping (triangles).

softens when the extent is large and approaches the lattice mode spectrum for the opposite limit [Fig. 3(b)].

Simultaneously, the DB amplitude, which can be identified with its dipole moment, varies substantially with varying size (Fig. 4), as anticipated from the fact that the spatial spread is determined by the central DB dipole size.

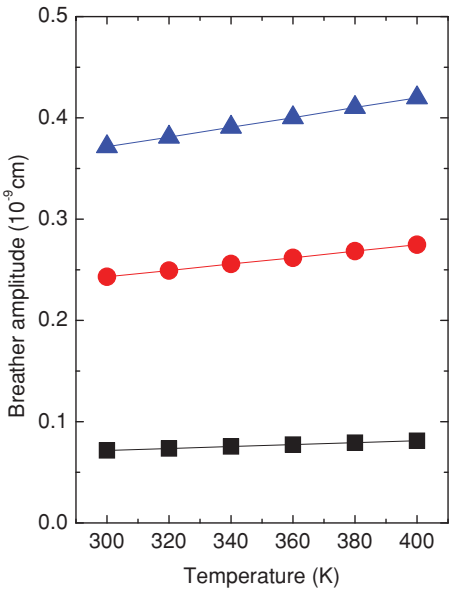

FIG. 4. (Color online) Temperature dependence of the breather amplitude for the case of dilute doping (squares), intermediately dense doping (circles), and dense doping (triangles).

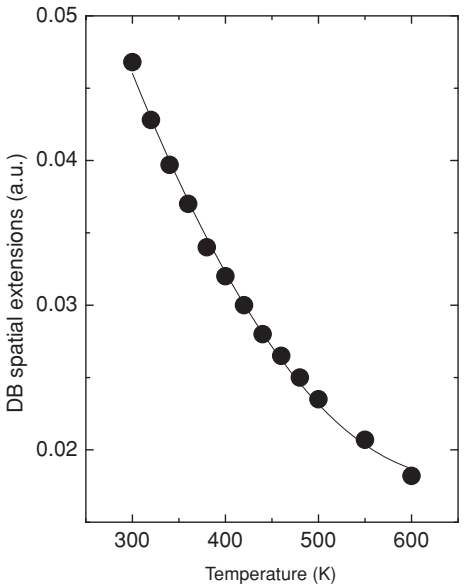

FIG. 5. Temperature dependence of the DB spatial extent for temperature-independent DB frequency.

Also, its temperature dependence changes with the spread, being almost constant for small amplitudes, while a linear T dependence sets in with increasing amplitude. Note that in the above the DB size has been set as constant and its frequency been calculated self-consistently. On the other hand, one could start from a T-independent frequency and calculate the DB-related length scale self-consistently. In this case the DB extent adopts a nonlinear T dependence with rapid growth upon decreasing the temperature (Fig. 5). Such a scenario has been suggested to be realized in some relaxors where a T-dependent growth of PNR's has been indirectly inferred experimentally.[8]

IV. COMPARISON WITH EXPERIMENTAL DATA

The above findings can be related to various experiments. Particularly, the emergence of an additional structure in the dielectric response has been frequently reported and attributed, as it is here, to PNR formation.[6–8] The acoustic mode anomalies that are present in this approach have been observed by Brillouin scattering and in measurements of the elastic constants.[8,36–42] The two-component behavior, characteristic for two time and length scales, has also been seen in NMR experiments.[15] Almost direct evidence for DB formation has been obtained recently by pulsed neutron inelastic scattering, where the emergence of a momentum-limited dispersionless mode has been observed.[12]

The theoretical picture developed here can be directly compared to recent extended data on the complex permittivity obtained for 0.2PSN-0.4PMN-0.4PZN ceramics, which are detailed below. These experiments have the advantage of covering a large frequency regime, which allows to detect coexisting regions of slow and fast dynamics.

In order to understand the dielectric relaxation in relaxors, it is more convenient to use frequency plots of the complex permittivity at various representative temperatures (see Fig. 6). A huge change in the dielectric dispersion takes place with

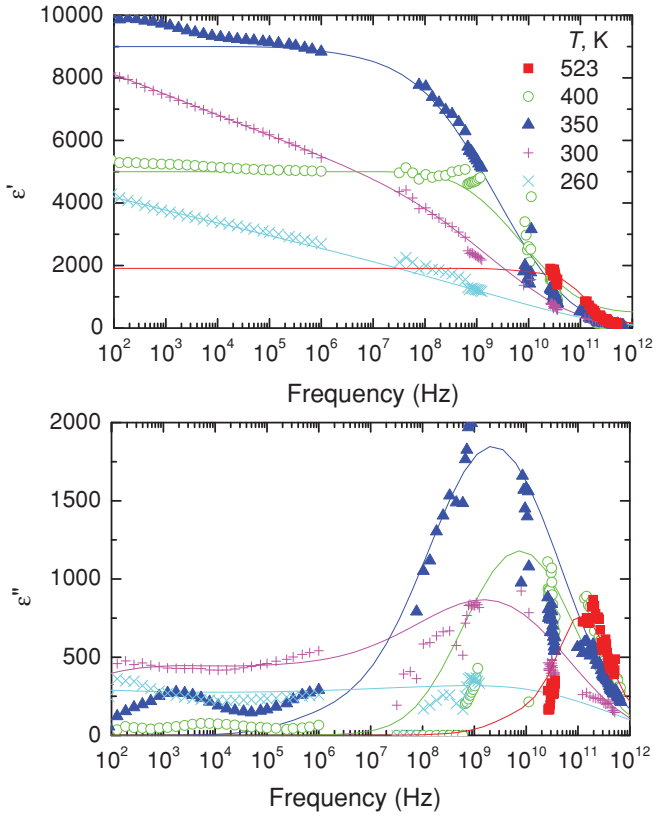

FIG. 6. (Color online) Frequency dependence of complex dielectric permittivity $\varepsilon', \varepsilon''$of 0.2PSN-0.4PMN-0.4PZN ceramics measured at different temperatures. The solid lines are the best fit with the distribution of the relaxation times.

decreasing temperature. At temperatures $T \geqslant 400$ K, the dielectric loss dispersion is clearly symmetric and observable only at frequencies larger than 1 GHz. On cooling, the relaxation slows down and broadens. At temperatures around 300 K the relaxation becomes strongly asymmetric and very broad. On further cooling, the dielectric dispersion broadens so tremendously that only part of it is visible in the available frequency range.

In order to determine the real and continuous distribution function of relaxation times $f(\tau)$ the Fredholm[44] integral equation is used:

$$\varepsilon'(\omega) = \varepsilon_\infty + \Delta\varepsilon \int_{-\infty}^{\infty} \frac{f(\tau)d(\ln\tau)}{1+\omega^2\tau^2}, \tag{3a}$$

$$\varepsilon''(\omega) = \Delta\varepsilon \int_{-\infty}^{\infty} \frac{\omega\tau f(\tau)d(\ln\tau)}{1+\omega^2\tau^2}, \tag{3b}$$

where the Tikhonov regularization method has been employed.[45–47] This method and calculation technique is described in detail elsewhere.[48]

The calculated distributions of the relaxation times $f(\tau)$are presented in Fig. 7. Symmetric and narrow distributions of relaxation times are observed at temperatures $T > 350$ K. On cooling, $f(\tau)$ adopts an asymmetric shape, and a second maximum appears at lower frequencies. The shortest and longest limits of $f(\tau)$ were calculated (level 0.1 of the maximum $f(\tau)$was chosen for the definition of the limits) at

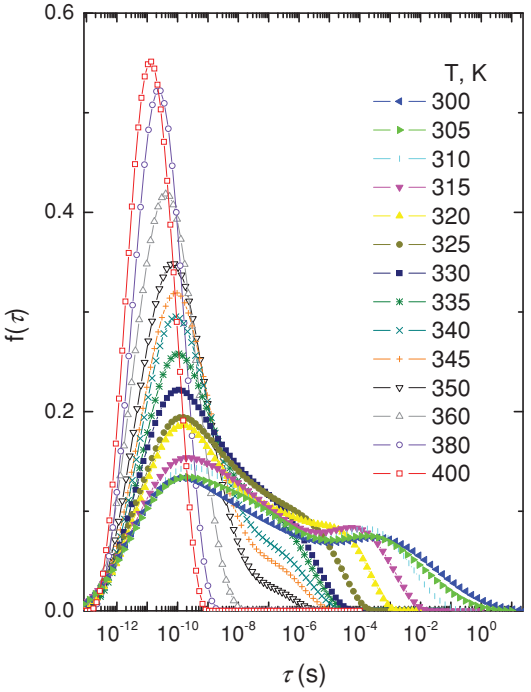

FIG. 7. (Color online) Distribution of relaxation times $f(\tau)$ of 0.2PSN-0.4PMN-0.4PZN ceramics calculated at different temperatures.

various temperatures (Fig. 8). The maximum relaxation time τ_{max} diverges according to the Vogel-Fulcher law:

$$\tau = \tau_0 e^{\frac{E_f}{k_B(T-T_0)}}, \tag{4}$$

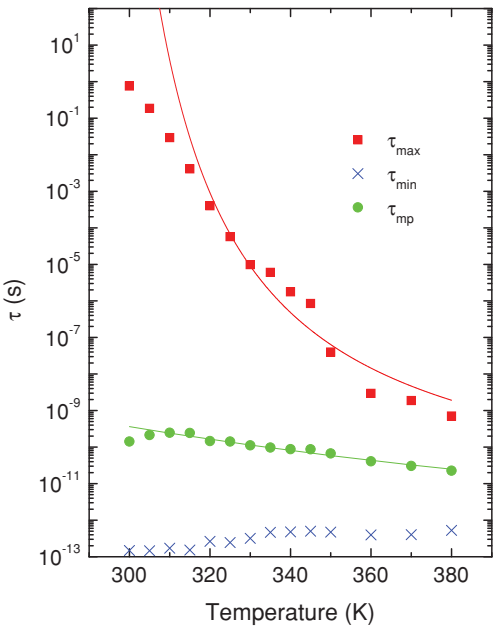

FIG. 8. (Color online) Temperature dependences of the longest τ_{max} (squares), most probable τ_{mp} (crosses), and the shortest τ_{min} (circles) relaxation times in 0.2PSN-0.4PMN-0.4PZN ceramics. Solid lines for τ_{max} are results of a Vogel-Fulcher fit and a linear interpolation for τ_{mp}.

where $\tau_0 = 10^{-12}$ s, $T_0 = 285$ K, and $E_f/k_B = 715$ K. All the shortest relaxation times have the same values, namely, 10^{-12}–10^{-13} s, and are almost temperature independent within the accuracy of this analysis. The most probable relaxation time $\tau_{\rm mp}$ obtained from the peak of distributions follows the Arrhenius law (Fig. 7):

$$\tau_{\rm mp} = \tau_0 e^{-\frac{E_A}{k_B T}}, \tag{5}$$

with parameters $\tau_0 = 1.06 \times 10^{-15}$ s and $E_A/k_B = 3825$ K.

The distribution function $f(\tau)$ was determined only at rather high temperatures, when the relaxation time lies within the experimental frequency range, whereas when $\tau_{\rm max}$ is below this range, neither the static permittivity nor $\tau_{\rm max}$ can be determined unambiguously. It can, however, be expected that $\tau_{\rm max}$ does not diverge below T_0 since some dispersion also remains below the freezing temperature. On the other hand, the Arrhenius law describes the temperature dependence of $\tau_{\rm mp}$ sufficiently well in the considered temperature range of 300–400 K. At higher temperatures ($T > 400$) this law breaks down since $\tau_{\rm max}$ is smaller than 10^{-13} s and stays almost constant for this temperature regime.

Even though the origin of the two-component dielectric relaxation is still under debate, it is interpreted here as arising from the DB formation and its interaction with the embedding matrix. The emergence of the low-frequency broad peak is identified with the DB mode frequency, which gains strength at the expense of the high-frequency response with decreasing temperature, in close analogy to our modeling (see Figs. 1 and 2). It has to be emphasized, however, that, experimentally, this peak appears in the very low frequency regime to shift to higher frequencies with increasing temperature, whereas, theoretically, the almost-static regime is not observed. Note that the high-frequency peak is not completely temperature independent but that a slight softening with decreasing temperature sets in, as predicted theoretically [Fig. 3(a)]. The overall qualitative agreement between experiment and theory thus confirms the picture developed in the introduction.

V. CONCLUSIONS

In conclusion, relaxor ferroelectrics have been modeled in terms of two components, which stem, however, from the same lattice dynamics. While one component exists on a short length scale, corresponding to PNR's, the second reflects the matrix in which the PNR's are embedded. The coupling between these stabilizes the lattice but adds a temperature dependence to the PNR's. The theoretical approach is supported by broadband dielectric spectroscopy, which agrees with the predicted behavior.

[1] G. Smolenski and A. Agarnovskaya, Sov. Phys. Solid State **1**, 1429 (1960).
[2] D. Viehland, S. J. Land, L. E. Cross, and M. Wuttig, J. Appl. Phys. **68**, 2961 (1990).
[3] C. Randall, Ph.D. thesis, University of Essex, 1987.
[4] L. E. Cross, Ferroelectrics **76**, 241 (1987).
[5] For a recent review see, G. A. Samara, J. Phys. Condens. Matter. **15**, R367 (2003), and references therein.
[6] J. Macutkevic, S. Kamba, J. Banys, A. Brilingas, A. Pashkin, J. Petzelt, K. Bormanis, and A. Sternberg, Phys. Rev. B **74**, 104106 (2006).
[7] S. Kamba, D. Nuzhnyy, V. Bovtun, J. Petzelt, Y. L. Wang, N. Setter, J. Levoska, M. Tyunina, J. Macutkevic, and J. Banys, J. Appl. Phys. **102**, 074106 (2007).
[8] S. Tsukada and S. Kojima, Phys. Rev. B **78**, 144106 (2008).
[9] P. M. Gehring, H. Hiraka, C. Stock, S.-H. Lee, W. Chen, Z.-G. Ye, S. B. Vakhrushev, and Z. Chowdhuri, Phys. Rev. B **79**, 224109 (2009).
[10] P. M. Gehring, S. Wakimoto, Z.-G. Ye, and G. Shirane, Phys. Rev. Lett. **87**, 277601 (2001).
[11] P. M. Gehring, S.-E. Park, and G. Shirane, Phys. Rev. B **63**, 224109 (2001).
[12] W. Dmowski, S. B. Vakhrushev, I.-K. Jeong, M. P. Hehlen, F. Trouw, and T. Egami, Phys. Rev. Lett. **100**, 137602 (2008).
[13] O. Svitelskiy, D. La-Orauttapong, J. Toulouse, W. Chen, and Z.-G. Ye, Phys. Rev. B **72**, 172106 (2005).
[14] I.-K. Jeong, T. W. Darling, J. K. Lee, Th. Proffen, R. H. Heffner, J. S. Park, K. S. Hong, W. Dmowski, and T. Egami, Phys. Rev. Lett. **94**, 147602 (2005).
[15] R. Blinc, V. Laguta, and B. Zalar, Phys. Rev. Lett. **91**, 247601 (2003).
[16] A. Simon, J. Ravez, and M. Maglione, J. Phys. Condens. Matter **16**, 963 (2004).
[17] M. Tyunina and J. Levoska, Phys. Rev. B **70**, 132105 (2004).
[18] J. Toulouse, P. DiAntonio, B. E. Vugmeister, X. M. Wang, and L. A. Knauss, Phys. Rev. Lett. **68**, 232 (1992).
[19] J. Toulouse and B. Hennion, Phys. Rev. B **49**, 1503 (1994).
[20] A. R. Bishop, A. Bussmann-Holder, S. Kamba, and M. Maglione, Phys. Rev. B **81**, 064106 (2010).
[21] S. Vakhrushev, S. Zhukov, G. Fetisov, and V. Chernychov, J. Phys. Condens. Matter **6**, 4021 (1994).
[22] G. Burns and F. H. Dacol, Solid State Commun. **48**, 835 (1983).
[23] V. Westphal, W. Kleemann, and M. D. Glinchuk, Phys. Rev. Lett. **68**, 847 (1992).
[24] R. Blinc, J. Dolinsek, A. Gregorovic, B. Zalar, C. Filipic, Z. Kutnjak, A. Levstik, and R. Pirc, Phys. Rev. Lett. **83**, 424 (1999).
[25] B. E. Vugmeister and P. Adhikari, Ferroelectrics **157**, 341 (1994).
[26] B. E. Vugmeister and M. D. Glinchuk, Rev. Mod. Phys. **62**, 993 (1990).
[27] J. Toulouse, B. E. Vugmeister, and R. Pattnaik, Phys. Rev. Lett. **73**, 3467 (1994).
[28] A. Bussmann-Holder and A. R. Bishop, Phys. Rev. B **70**, 184303 (2004).
[29] A. Bussmann-Holder, A. R. Bishop, and T. Egami, Europhys. Lett. **71**, 249 (2005).
[30] A. Bussmann-Holder and A. R. Bishop, J. Phys. Condens. Matter **16**, L313 (2004).
[31] R. Migoni, H. Bilz, and D. Bäuerle, Phys. Rev. Lett. **37**, 1155 (1976).

[32]H. Bilz, G. Benedek, and A. Bussmann-Holder, Phys. Rev. B **35**, 4840 (1987).
[33]A. Bussmann-Holder and H. Büttner, Nature (London) **360**, 541 (1992).
[34]G. Benedek, A. Bussmann-Holder, and H. Bilz, Phys. Rev. B **36**, 630 (1987).
[35]A. Bussmann-Holder, A. R. Bishop, and G. Benedek, Phys. Rev. B **53**, 11521 (1996).
[36]S. G. Lushnikov, A. I. Fedoseev, S. N. Gvasaliya, and S. Kojima, Phys. Rev. B **77**, 104122 (2008).
[37]R. Laiho, S. G. Lushnikov, S. D. Prokhorova, and I. G. Siny, Sov. Phys. Solid State **32**, 2024 (1990).
[38]I. G. Siny, S. G. Lushnikov, C.-S. Tu, and V. H. Schmidt, Ferroelectrics **170**, 197 (1995).
[39]S. G. Lushnikov, J.-H. Ko, and S. Kojima, Appl. Phys. Lett. **84**, 4798 (2004).
[40]M. Ahart, A. Asthagiri, Z.-G. Ye, P. Dera, H.-K. Mao, R. E. Cohen, and R. J. Hemley, Phys. Rev. B **75**, 144410 (2007).
[41]G. A. Smolenski, N. K. Yushin, and S. I. Smirnov, Sov. Phys. Solid State **27**, 801 (1985).
[42]A. Kohutych, R. Yevych, S. Perechinskii, V. Samulionis, J. Banys, and Yu. Vysochanskii, Phys. Rev. B **82**, 054101 (2010).
[43]For a recent review, see Ref. 5 and A. A. Bokov and Z.-G. Ye, J. Mater. Sci. **41**, 31 (2006).
[44]H. Schäfer, E. Sternin, R. Stannarius, M. Arndt, and F. Kremer, Phys. Rev. Lett. **76**, 2177 (1996).
[45]A. N. Tikhonov and V. Y. Arsenin, *Solution of Ill-Posed Problems* (Wiley, New York, 1977).
[46]C. W. Groetsch, *The Theory of Tikhonov Regularization for Fredholm Equations of the First Kind* (Pitman, London, 1984).
[47]S. W. Provencher, Comput. Phys. Commun. **27**, 213 (1982).
[48]J. Macutkevic, J. Banys, and A. Matulis, Nonlinear Anal. Model. Control **9**, 1 (2004).